Hindawi
International Transactions on Electrical Energy Systems
Volume 2024, Article ID 9687002, 14 pages
https://doi.org/10.1155/2024/9687002

Research Article

Providing a New Multiobjective Two-Layer Approach for Developing Service Restoration of a Smart Distribution System by Islanding of Faulty Area

Hasan Keshavarz Ziarani,[1] **Seyed Hossein Hosseinian**,[2] **and Ahmad Fakharian**[1]

[1]*Department of Electrical Engineering, Qazvin Branch, Islamic Azad University, Qazvin, Iran*
[2]*Department of Electrical Engineering, Amirkabir University of Technology, Tehran, Iran*

Correspondence should be addressed to Ahmad Fakharian; ahmad.fakharian@qiau.ac.ir

Received 3 April 2023; Revised 20 October 2023; Accepted 14 December 2023; Published 2 January 2024

Academic Editor: Michele De Santis

One of the essential capabilities of a smart distribution network is to improve network restoration performance using the postfault islanding method. Islanding of the faulty area can be done offline and online. Online islanding will decrease load shedding and operation cost. In this study, a novel two-step mathematical method for system restoration after the fault is presented. A new mathematical model for the optimal arrangement of the system for the faulty area in the first layer is proposed. In this layer, the main objective is to decrease the distribution system's load shedding and operational costs. In this regard, after the fault event, the boundary of the islanded MGs is determined. Then, in the second layer, the problem of unit commitment in the smart distribution network is addressed. In addition to the load shedding, optimal planning of energy storage systems (ESSs) and nondispatchable distributed generation (DG) resource rescheduling are also determined in this layer. The important advantages of the proposed approach are low execution time and operational costs. A demand response (DR) program has also been used for optimal system restoration. Solving the problem using the multiobjective method with the epsilon-constraint method is another goal of the paper, which simultaneously minimizes the cost and the emissions of the smart distribution network. The proposed model has been tested on an IEEE 33-bus system. Better performance of the proposed model compared to the techniques in the literature has been proven.

1. Introduction

To develop renewable resources and reduce concerns about the problem of environmental pollution and the increasing use of the smart grid, government incentives aimed at developing distributed generations and implementing demand response programs have a significant effect. Some smart grid goals include the following: participation of distributed generation resources at the distribution network level, the use of electrical storage resources to participate in DR programs, responding to real-time loads and prices, self-healing, and smart protection.

One of the important capabilities of smart grids is service restoration in the event of a fault in the power systems. Optimal restoration is carried out with the aim of minimizing load shedding. Also, all system constraints should be considered. The system's ability to quickly detect faults, take necessary actions to reduce the adverse effects of faults, and quickly restore the system to a stable operating state is defined as self-healing [1]. The structure of the smart grid, while implementing the self-healing strategy, is categorized into smart transmission grid, smart distribution grid, and smart MGs [2]. The method of differential evolution algorithm is chosen in [3] to optimize the performance of network MGs in self-healing mode. The evolving search space method for new configurations is performed by combining graph theory and a heuristic method [4]. To restore service to the maximum customers affected due to the contingency, a fuzzy multiagent system was used in the distribution system [5]. In [6], an adaptive restoration

decision support system based on a two-step MILP problem has been used to address the challenging online restoration problem. In [7], a self-healing control strategy is proposed that includes fault detection, fault localization, faulted area isolation, and power restoration in the electrical distribution system. In [8], a voltage control method is presented based on a comprehensive architectural model consisting of several distributed photovoltaic resources and management systems that support network reconfiguration after the self-healing operation. A self-healing approach is presented in [9], which evaluates the robustness of networked MGs during the islanded mode. Network flexibility and resilience are essential in risky events such as bad weather conditions and cyberattacks. A mixed-integer linear optimization method is proposed to achieve self-healing operation to minimize load shedding [10]. Concepts related to the self-healing capability of smart grids include transmission, distribution, MGs, transient stability, and cyberattack [11].

In many studies, the process of energy distribution system management has been investigated. The optimal model for self-healing management in active distribution systems, including electric vehicles (EVs), renewable energy sources, and DR programs, is presented in [10]. In [12], with the aim of day-ahead planning of a smart distribution system, a comprehensive operating method has been made for normal and emergency conditions. In [13], the daily optimal scheduling problem of networked MGs using a metaheuristic algorithm under uncertainties of renewable energy systems and loads is investigated in a proposed energy management system. In [14], the authors have studied the energy consumption management of a rural MG in the optimization framework based on a new stochastic method to balance generation and demand.

Recently, DR programs have been converted into an essential interest for researchers. A variety of loads, such as industrial, commercial, and residential, in the DR programs, can help to introduce them as flexible and smart loads [15]. The authors in [16] have investigated the effect of DR programming simultaneously with the multi-MG-based operation of smart distribution systems. A step-wise DR program has been used in the energy management system for an isolated structure of networked MGs. Scenario-based analysis has dealt with the uncertainty of renewable energy sources and loads [17]. In [18], an ESS, an MG consisting of a combined heating and cooling system, photovoltaic power generation, and the response load are implemented to check the optimal scheduling process of these units. In [19], the effectiveness of DR programs and local load energy supply by microgrid based on renewable resources has been studied. The authors in [20] present a method to evaluate the way of real-time energy management in smart grids. A multi-objective approach is used to implement a DR program considering the power grid's load factor and residential users' energy costs [21]. In [22], an energy management toolbox for the buildings connected to the electric grid has been modeled.

Various studies have dealt with faults in the self-healing mode and focused on island building. In [23], the effect of EVs on improving the self-healing properties in an islanding mode in the power grid is evaluated. A real-time self-healing scheme with measurement and model-based algorithms has been proposed [24] to deal with severe power system disturbances.

An MG is a structure that can be connected or disconnected from the main grid. MGs are usually switched to the islanded mode due to economic problems, maintenance purposes, and network faults. When an outage occurs, MGs can operate in islanded mode or grid-connected mode. MGs downstream of the grid can act as a standalone source for their customers by disconnecting from the network [25]. In [26], an optimal self-healing method for MG islanding under different scenarios has been investigated, an islanded MG optimization scheduling focused on frequency adjustment of units, and DR is proposed. A novel concept of conventional droop control is developed as a fast droop controller in [27] cooperation with a modern frequency controller to ensure the reliability of the microgrid system. In [28], an optimal integral proportional control method is used in an island microgrid. The different categories for intentional islanding of MG at the point of standard coupling have been analyzed in [29]. In the self-healing scheme for the reconfiguration of smart distribution networks with the presence of DGs, a heuristic algorithm with a tree structure is used [30]. An energy management system with convex relaxation has been developed in [31] for an islanded MG that optimizes its operating cost. An optimal method for energy management is used in [32], which increases the reliability of an MG structure and considers the profit of small network owners. A comprehensive study of different MG control methods, such as hierarchical control of the islanded MGs, has been carried out in [33].

There are various methods to optimize the energy management of MGs by considering the technical constraints, which can be mentioned using mathematical approaches or heuristic optimization techniques. A mathematical approach for enhancing the resiliency of the MG energy management system, based on islanded mode, has been developed [34]. In [35], a mathematical model for renewable energy penetration in an island MG, in the presence of DR and ES, is proposed to mitigate the imbalance of supply and demand due to the intermittent nature of renewable production. The authors in [36] provide an overview of optimization and mathematical modeling of the DR algorithm and its implementation at various levels in the smart grid. The study in [37] proposes a performance analysis of power system parameters, including the voltage, frequency, real and reactive power, and phase angle, to detect the island using mathematical morphology. In [38], a new strategy for MG protection based on mathematical morphology is introduced. The proposed scheme was investigated for islanded systems and grid connected with loop and radial configurations. In [39], a two-step method is used that, in the first layer, solves a mixed-integer linear programming (MILP) problem and, in the second layer, solves a nonlinear programming (NLP) problem. In [40], a two-stage stochastic program has been used, which optimizes the output power of WTs and PVs and load consumption in the first stage and adjusts production in the second stage with

suitable scenarios based on the output power of renewable sources. In [41, 42], a two-step method is used. In the first step, graph theory integrated with the binary particle swarm optimization (PSO) algorithm is utilized to determine the optimal arrangement of the distribution system. In the second step of a nonlinear model, the unit commitment problem is solved mathematically [41]. The models presented in [39–42] have a very high execution time due to their nonlinearity, and it is practically impossible to use these models in large systems. On the other hand, due to intelligent algorithms, achieving the optimal solution will not be guaranteed. However, in the present study, a new linearized two-step method is used. The proposed model is solved using mathematical solvers. The proposed model also uses a load-shedding tool integrated with DR schemes, while, in [39–42], DR-based methods were not used.

The online island construction method retrieves the service in the fault zone in the proposed scheme. In the online islanding manner, the boundaries of island MGs and the number of MGs are determined optimally after the fault in a part of the distribution system. After the fault occurs, the fault line is isolated. Then, the optimal island MG is determined by closing the tie switches and opening switches in the faulty area. In addition to creating an optimal island operation, the radial condition of the system is maintained. Therefore, several tie switches may be closed, and several switches may be opened. Of course, upstream network switches are not in planning optimal MG configuration in the faulty area. Because the faulty area will be connected to the upstream network, the system will no longer act as an island. While in the proposed method, the performance of the system in the faulty area is considered based on the formation of one/multiple islands. Therefore, in the first layer, islanded MGs will be formed via the formation of optimal MGs using a linear mathematical model. In the second layer, the unit commitment problem of smart distribution systems is solved by the optimal arrangement formed in the first step. At this stage, the unit commitment problem integrated with load-shedding tools and DR schemes is solved mathematically using a linear model. One of the advantages highlighted by the proposed method is using an optimal approach that can significantly decrease the execution time of the problem and achieve an optimal solution. Also, in the proposed model, all possible tools, such as smart load shedding, DR, various DG resources, and ESS, have been used for optimal restoration.

Another issue that we will discuss in this study is emissions. In multiobjective modeling, the increase in investors' profits, along with the reduction of environmental pollutants, has become more prominent. Therefore, a solution that only maximizes the total profit or minimizes the total scheduling costs may not be suitable for power grids alone. Thus, the multiobjective framework is proposed for solving the problem mentioned above, considering emissions. The multiobjective method is used in articles, such as [43, 44], to maximize profits and minimize emissions. The authors in [43] investigate the role of the renewable-based VPP in maximizing profit and minimizing emissions in a two-objective manner. The authors in [44] solve the bilevel problem with the augmented epsilon-constraint method in a biobjective way, which minimizes the emission of virtual power plant units and maximizes the profit. In the epsilon-constraint method, the primary objective function is designated the leading objective, while the second to n-th objectives are constrained to a specific maximum value. Altering this value can result in multiple solutions, some of which may not exhibit efficiency. It should be noted that none of the papers devoted to solving the problem of service restoration of a smart distribution network has incorporated multiobjective issues.

The main components of the article are described as follows:

(i) Providing a novel mathematical model for solving the reconfiguration problem of a smart distribution system after a fault.

In literature, intelligent algorithms, graph theory, and nonlinear models have mainly been used in the first layer. However, this paper uses a new linear model for reconfiguration after the fault. The proposed model leads to a decrease in the solution time and optimal solutions.

(ii) Solving the unit commitment problem in a smart distribution system with smart load shedding and DR tools.

In the second layer, the unit commitment problem is solved by DG rescheduling and responsive loads. The proposed linear model leads to an optimal response at low solution times like the first layer. Execution time is essential in the restoration problem.

(iii) Creating optimal islanded MGs in the faulty area.

Another advantage of the proposed method is the creation of optimal MGs after the fault; while, in the methods with the islanding approach in the literature, MGs are formed offline. Online formation of MGs is essential because, according to the available resources and the fault location, the boundaries of MGs are formed, which will lead to a reduction in load shedding of the distribution systems.

(iv) Providing mathematical modeling and new objective functions for the restoration problem of the smart distribution system problem.

(v) A multiobjective model is introduced to minimize the cost and emission in the smart distribution network based on the epsilon-constraint method.

In the following, two-layer linear mathematical modeling is used. The formulation of the model is described in Section 3. Section 4 is related to case studies and results, and finally, in the last section, the conclusion is presented.

2. Proposed Approach

The assumptions for optimizing the problem according to the study of references [19, 22, 23, 45] are mentioned as follows:

(i) The system under consideration is balanced.

(ii) Reactive load distribution is omitted.

(iii) The penetration factor of microturbines (MTs) is considered to be one. This means that they cannot work in overload conditions.

(iv) There are energy storage and dispatchable and nondispatchable DG in a smart distribution network. Storage is essential in smart distribution systems because these resources, due to their very high response speed, can overcome the uncertainty of nondispatchable DG resources. Another factor in a smart distribution network is the ability to run DR programs. In this paper, DR is used for the optimal restoration of distribution systems. In this paper, home devices are divided into two categories: uncontrollable devices and controllable devices. Controllable devices are divided into shiftable loads as the first priority, interruptible loads as the second priority, and adjustable loads as the third priority. Shiftable loads (first priority), such as a microwave, can be transfered for use another time. When these devices start working, they should continue to work without stopping until their work cycle is completed. Interruptible loads (second priority), such as a vacuum cleaner, can also be interrupted at any time. Adjustable loads (third priority) such as a refrigerator can be reduced in emergency situations.

In this paper, a two-step algorithm is presented. In the first step, the restoration of the distribution system is achieved by a new linear model. In the second step, the unit commitment problem of distribution systems is solved by the optimal arrangement created in the first step. Then, the load-shedding tool is used on responsive loads. Rescheduling of dispatchable DG resources is also carried out. If the condition of balance is not met through the reduction of responsive loads and rescheduling of DG resources, the load will be curtailed. Of course, load shedding with high priority will impose more costs on the operation of distribution systems. The proposed solution algorithm is shown in Figure 1.

3. Formulation

This step presents a novel objective function to solve the restoration problem. In objective function (1), term 1 is the penalty for voltage deviation from the allowable amount. In this term, the values are in the form of per unit. The c^{delv} is the voltage deviation coefficient penalty in dollars. Term 2 is the profit from the sale of electricity to customers. Terms 3 to 6 show the cost of load shedding of the first, second, and third priorities and load outage, respectively. Power flow in the lines of each MG is described in term 7. $x(k.j) = 0$ does not mean the line will be cut, but rather that the current on the line can be zero. In other words, $x(k.j) = 0$ means the line between the buses and is a candidate of boundary lines between two self-adequate MGs with minimized generation-load imbalance [40].

This item minimizes the total number of connected lines that lead to island MGs.

$$\text{Min} \sum_t \left(\sum_{k,t} c^{\text{delv}} \left| \Delta V_{k,t} \right| - \sum_k c^D p^D_{k,t} + \sum_k c^{\text{LS1}} P^{\text{LS1}}_{k,t}(k,t) + \sum_k c^{\text{LS2}} P^{\text{LS2}}_{k,t}(k,t) + \sum_k c^{\text{LS3}} P^{\text{LS3}}_{k,t}(k,t) + \sum_k c^{\text{LS4}} P^{\text{LS4}}_{k,t}(k,t) + \sum_{k,j} x(k,j) \right). \quad (1)$$

In the first term, the voltage may deviate higher or lower than the nominal voltage. Therefore, the absolute value must be used. If the absolute value of the objective function is not used, the minimum allowable voltage should be used. Since the absolute value causes the model to be nonlinear, the absolute value must be converted to a linear relationship. In the first term of equation (2), the value $\text{xp}(k,t) + \text{xn}(k,t)$ is substituted. There are two positive variables. These two variables can be converted from a nonlinear model to a linear model by modeling the value of voltage deviation with the help of equation (3).

$$\text{Min} \sum_t \left(\sum_{k,t} c^{\text{delv}} (\text{xp}(k,t) + \text{xn}(k,t)) - \sum_k c^D p^D_{k,t} + \left(\sum_k c^{\text{LS1}} P^{\text{LS1}}_{k,t}(k,t) + \sum_k c^{\text{LS2}} P^{\text{LS2}}_{k,t}(k,t) + \sum_k c^{\text{LS3}} P^{\text{LS3}}_{k,t}(k,t) + \sum_k c^{\text{LS4}} P^{\text{LS4}}_{k,t}(k,t) \right) + \sum_{k,j} x(k,j) \right), \quad (2)$$

$$\Delta V_{k,t} = \text{xp}(k,t) - \text{xn}(k,t). \quad (3)$$

The following equation shows the allowable voltage value on each bus:

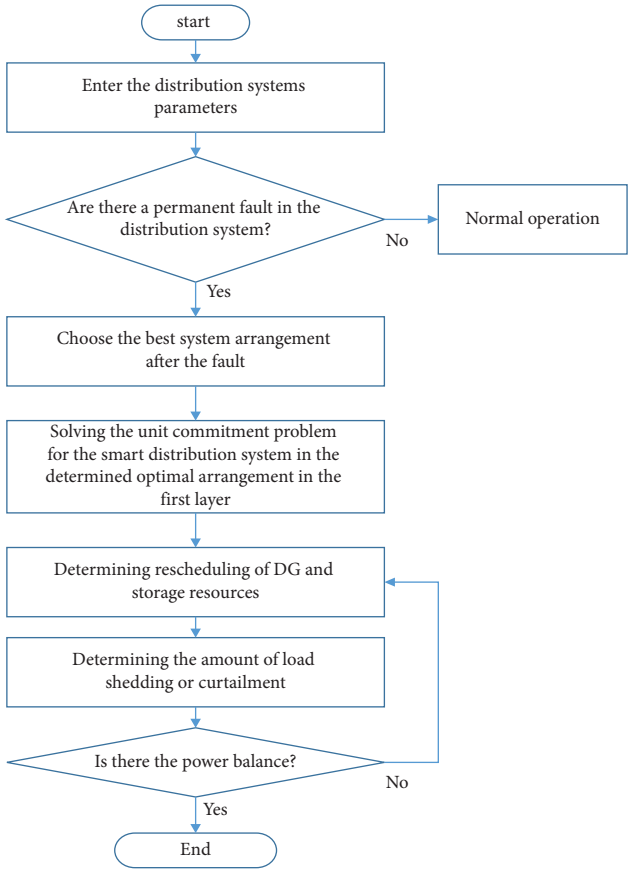

Figure 1: Proposed flowchart.

$$1 - \Delta v \le V_{k,t} \le 1 + \Delta v. \tag{4}$$

The active power flow equation is expressed in equation (5). This relationship is nonlinear and makes the solver not reach the desired answer. For this reason, the continuation of the formulation of this relation will be linear.

$$P_{k,j,t} = X_{k,j}\left(V_{k,t}\sum_{j} V_{j,t}\left(G_{k,j}\cos\theta_{kj,t} + B_{k,j}\sin\theta_{kj,t}\right)\right), \quad \forall k. \tag{5}$$

Due to the nonlinearity of the power flow equations in (5) and (6), these two relations are linearized as follows. To linearize, the following assumptions must be met:

(i) The voltage is always close to the nominal value.

(ii) The voltage angle difference is negligible. Therefore, $\sin\theta_k = \theta_k$ and $\cos\theta_k = 1$ can be considered.

Therefore, the voltage of a bus can be expressed as follows:

$$V_{k,t} = 1 + \Delta V_{k,t}. \tag{6}$$

Voltage changes must be within the allowable range ($\Delta V^{\min} \le \Delta V_k \le \Delta V^{\max}$). Therefore, according to equations (5)–(7), they change as follows:

$$P_{k,j,t} = \sum_{j}\left(1 + \Delta V_{k,t} + \Delta V_{j,t}\right)\left(G_{k,j} + B_{k,j}.\theta_{kj,t}\right), \quad \forall k. \tag{7}$$

Due to the multiplication of the two variables, equations (8) and (9) are still nonlinear. Since numerical results $\Delta V_{k,t}.\theta_{kj,t}$ and $\Delta V_{j,t}.\theta_{kj,t}$ are expected to be very insignificant. Therefore, these nonlinear terms are removed from equation (8), which are finally equation (10) linear relation of the power flow equation.

$$P_{k,j,t} = \sum_{j}\left(\left(1 + \Delta V_{k,t} + \Delta V_{j,t}\right)G_{k,j} + B_{k,j,t}.\theta_{\mathrm{kj},t}\right), \quad \forall k. \tag{8}$$

The transmission power of each line exists if the switch is closed ($X_{k,j} = 1$) and should be zero if the switch is open ($X_{k,j} = 0$). For this reason, by using the large M method and multiplying this binary variable by the injected active power in relation (9), this condition will be guaranteed.

$$P_{k,j,t} \le M \times X_{k,j}. \tag{9}$$

The active power balance equation can be seen in the following equation:

$$P_{k,j,t} = p^{G}_{k,t} + p^{E}_{k,t} - p^{D}_{k,t} + p^{\mathrm{WT}}_{k,t} + p^{\mathrm{PV}}_{k,t} + p^{\mathrm{ESc}}_{k,t} - p^{\mathrm{ESd}}_{k,t}. \tag{10}$$

The battery storage at low-load times helps to reduce the load shedding on the distribution system by storing energy and discharging during peak times. In the below, the limit of discharge and charge is represented.

$$-P^{\mathrm{ch,max}}_{k}\lambda_{k,t} \le p^{E}_{k,t} \le P^{\mathrm{dch,max}}_{k}\phi_{k,t}. \tag{11}$$

The battery storage can only be discharged or charged by the following equation:

$$\lambda_{k,t} + \phi_{k,t} \le 1. \tag{12}$$

The battery charging mode is mentioned in the following equation:

$$\mathrm{SOC}_{k,t} = \mathrm{SOC}_{k,t-1} - \frac{T}{\mathrm{EC}_k}\left(\phi_{k,t}p^{E}_{k,t}\pi_d^{-1} + \lambda_{k,t}p^{E}_{k,t}\pi_c\right). \tag{13}$$

The minimum and maximum battery charge statuses are expressed as follows:

$$0 \le \mathrm{SOC}_{k,t} \le \mathrm{SOC}^{\max}_{k}. \tag{14}$$

The operating range related to the output power of MTi at time t is given in (15).

$\underline{\mathrm{pg}}_{(k,t)}$ and $\overline{\mathrm{pg}}_{(k,t)}$ express the minimum and maximum time-dependent operating range, respectively. It is not necessary that two variables are equal to $\mathrm{pg}^{\min}_{k,t}$ and $\mathrm{pg}^{\max}_{k,t}$.

The lower and upper limits of operation $\underline{\mathrm{pg}}_{(k,t)}$ and $\overline{\mathrm{pg}}_{(k,t)}$ are described in (16) and (18). The up/down level constraints of MT ramps are shown in relations (17) and (19).

$$\underline{\mathrm{pg}}_{(k,t)} \le \mathrm{pg}_{(k,t)} \le \overline{\mathrm{pg}}_{(k,t)}, \tag{15}$$

$$\overline{\mathrm{pg}}_{(k,t)} \le \mathrm{pg}_{k,t}^{\max}\left[u_{k,t} - z_{k,t+1}\right] + \mathrm{SD}_k z_{k,t+1}, \tag{16}$$

$$\overline{\mathrm{pg}}_{(k,t)} \le \mathrm{pg}_{(k,t-1)} + \mathrm{RU}_k u_{k,t-1} + \mathrm{SU}_k y_{k,t}, \tag{17}$$

$$\underline{\mathrm{pg}}_{(k,t)} \ge \mathrm{pg}_{k,t}^{\min} u_{k,t}, \tag{18}$$

$$\underline{\mathrm{pg}}_{(k,t)} \le \mathrm{pg}_{(k,t-1)} + \mathrm{RD}_k u_{k,t} + \mathrm{SD}_k z_{k,t}. \tag{19}$$

In (20) and (21), the costs related to the shutdown and start-up of MTs are stated. These costs are used in the planning of MTs and the objective function in (1) and (2).

$$\mathrm{SDC}(k,t) = \mathrm{sd}_k\, z_{k,t}, \tag{20}$$

$$\mathrm{STC}(k,t) = \mathrm{su}_k\, y_{k,t}. \tag{21}$$

The on-off status of unit i at time t is determined by $u_{i,t}$. The shutdown and start-up of MTs are also represented by $z_{i,t}$ and $y_{i,t}$. On and off constraints of MTs are described in (22) and (23), respectively. However, these two relations make the model to a nonlinear model. To linearize the minimum shutdown limit, linearized relations (24)–(26) instead of (22) are used. In (24), the shutdown and start-up of the MT are limited to the MTs on-off state in the last time. Equation (25) shows that the MT turns off or on at time t, and both states cannot occur simultaneously. Equation (26) also indicates that $u_{i,t}$, $y_{i,t}$, and $z_{i,t}$ are binary variables.

$$\left(y_{k,t-1} - \mathrm{UT}_k\right) \times \left(u_{k,t-1} - u_{k,t}\right) \ge 0, \tag{22}$$

$$\left(y_{k,t-1} - \mathrm{DT}_k\right) \times \left(u_{k,t} - u_{k,t-1}\right) \le 0, \tag{23}$$

$$y_{k,t} - z_{k,t} = u_{k,t} - u_{k,t-1}, \tag{24}$$

$$y_{k,t} + z_{k,t} \le 1, \tag{25}$$

$$y_{k,t}, z_{k,t}, u_{k,t} \in \{0,1\}. \tag{26}$$

Equations (27)–(30) represent the minimum stay-on limit of each MT.

$$\sum_{t=1}^{\xi_i}\left(1 - u_{k,t}\right) = 0, \tag{27}$$

$$\sum_{t=\Gamma}^{\Gamma+\mathrm{UT}_k-1} u_{k,t} \ge \mathrm{UT}_k y_{k,\Gamma}, \forall\, \Gamma = \xi_k + 1, \ldots, T - \mathrm{UT}_k + 1, \tag{28}$$

$$\sum_{t=\Gamma}^{T} u_{k,t} - y_{k,t} \ge 0, \forall\, \Gamma = T - \mathrm{UT}_k + 2, \ldots, T, \tag{29}$$

$$\xi_k = \min\left\{T, \left(\mathrm{UT}_k - U_k^0\right)u_{k,t}\right\}. \tag{30}$$

Equations (31)–(34) also indicate the minimum shutdown time of each MT.

$$\sum_{t=1}^{\xi_k} u_{k,t} = 0, \tag{31}$$

$$\sum_{t=\Gamma}^{\Gamma+\mathrm{DT}_i-1}\left(1 - u_{k,t}\right) \ge \mathrm{DT}_k\, z_{\mathrm{k},\Gamma}, \quad \forall\, \Gamma = \xi_k + 1, \ldots, T - \mathrm{DT}_k + 1, \tag{32}$$

$$\sum_{t=\Gamma}^{T} 1 - u_{k,t} - z_{k,t} \ge 0, \quad \forall\, \Gamma = T - \mathrm{DT}_\Gamma + 2, \ldots, T, \tag{33}$$

$$\xi_k = \min\left\{T, \left(\mathrm{DT}_k - S_k^0\right)\left[1 - u_{k,t=0}\right]\right\}. \tag{34}$$

The load power in each bus ($p_{i,t}^D$) consists of the total power of home appliances based on different priorities as follows (35).

The task of the load collector is to combine the power of the devices of different priorities on different buses and, at any moment, give the total energy of the distribution network in each priority to the DSM controller. Equation (36) shows that the whole load shedding by the priority on each bus is less than the total power of the priority device 1 of all the houses on each bus. Equations (37) and (38) also show the load-shedding constraints for priority loads 2 and 3, respectively. Equation (39) shows the load outage of uncontrolled loads.

$$p_{k,t}^D = \mathrm{Pload1}_{k,t}^D + \mathrm{Pload2}_{k,t}^D + \mathrm{Pload3}_{k,t}^D + \mathrm{Pload4}_{k,t}^D, \tag{35}$$

$$0 \le P_{k,t}^{\mathrm{LS1}} \le \mathrm{Pload1}_{k,t}^D, \tag{36}$$

$$0 \le P_{k,t}^{\mathrm{LS2}} \le \mathrm{Pload2}_{k,t}^D, \tag{37}$$

$$0 \le P_{k,t}^{\mathrm{LS3}} \le \mathrm{Pload3}_{k,t}^D, \tag{38}$$

$$0 \le P_{k,t}^{\mathrm{LS4}} \le \mathrm{Pload4}_{k,t}^D. \tag{39}$$

However, the unit commitment problem in the new system must be resolved after the restoration. At this stage, planning is carried out for dispatchable DG and ESS resources. Also, the amount of load shedding is determined at this step.

In the objective function of the second layer, all the practical objectives in modeling the problem of unit commitment problem are considered. In the objective function (40), the first to third terms show the cost of production and shutdown and start-up of MTs. Term 4 shows the profit of

customers' sales. Terms 5 to 8 show the cost of load shedding based on priorities 1 to 3 and load outage. The cost of buying electricity from the upstream network is stated in term 9, and the profit from the sale of electricity to the upstream network is stated in term 10. The generation cost of MTs is considered in some studies as a quadratic function. However, in [42], a linear model has been used for the production cost function of MTs due to computational load reduction. Therefore, in the objective function, instead of this nonlinear term, a linear term is used in relation.

$$f_1 = \text{Min} \sum_t \left(\sum_i c^G P_{i,t}^G + \sum_i \text{STC}(i,t) + \sum_i \text{SDC}(i,t) - \sum_i c^D P_{i,t}^D + \sum_i c^{\text{LS1}} P_{i,t}^{\text{LS1}} + \sum_i c^{\text{LS2}} P_{i,t}^{\text{LS2}} + \sum_i c^{\text{LS3}} P_{i,t}^{\text{LS3}} + \sum_i c^{\text{LC}} P_{i,t}^{\text{Lc}} \right) + C_t^b \lambda_t - C_t^s \mu_t. \tag{40}$$

In equation (41), the active power flow is represented. However, here, $x(k, j)$ is constant and indicates the status of the system lines resulting from the first step. Therefore, this relation no longer needs to be linearized by equation (9).

$$P_{k,j,t} = x(k,j) \times \sum_j \left(\left(1 + \Delta V_{k,t} + \Delta V_{j,t}\right) G_{k,j} + B_{k,j,t}.\theta_{kj,t} \right), \quad \forall k. \tag{41}$$

The second step equations are equations (8) and (10)–(40) that index i should be used instead of index k.

3.1. Multiobjective Modeling. The emission of the smart distribution systems is formulated based on a linear equation (42). The total production of each unit is multiplied by a fixed factor to obtain the emission value of the unit, which is shown in Table 1 [43].

$$f_2 = \sum_t \sum_i \varphi_i \times p_{i,t}^G. \tag{42}$$

In the problem of multiobjective mathematical programming, in most cases, there is a conflict between the objectives, that is, the improvement of the result of one of the objectives leads to the deterioration of the results of the other objectives. Therefore, the main difference between multiobjective and single-objective problems is that there is no single optimal solution in multiobjective problems that optimize all objectives simultaneously [44].

3.1.1. Epsilon-Constraint Method. The epsilon-constraint method is described below to solve a multiobjective optimization problem.

$$\begin{aligned} &\text{Min } f_1(x), \\ &\text{subject to } f_2(x) \le e_2. \end{aligned} \tag{43}$$

In the two-objective problem of emission and cost of the units, acts as the main objective function, which is the system cost, and emission ($f_2(x)$) act as a constraint. In addition, x is an array of decision variables, which in this problem are the generation power of units. By changing the e_2, Pareto solutions to the problem are generated (in this problem, there are 10 Pareto solutions) [45]. To solve the epsilon-constraint method, the problem is solved as a single objective by considering the main objective function (cost). In this case, cost is at its lowest amount, and the emission is at its highest amount. Then, emission is solved as a single objective. As a result of this, the emission is at its lowest value, and the cost is at its highest value. Then, to generate Pareto solutions, the model is solved as a single-objective problem by considering the cost as a main objective function and emission as a subobjective function (constraint) as shown in equation (43). By changing the amount of e_2, Pareto solutions are generated.

3.1.2. Fuzzy Decision-Making Method. By accessing all the Pareto solutions after solving the problem, the decision-maker should choose one of the Pareto solutions according to the prioritization and as the final solution. To choose the best answer for the decision-maker, it is suggested to use the fuzzy method with a linear membership function [43]. The proposed fuzzy decision-making method and its membership functions are defined as (44) and (45), used for maximization and minimization, respectively. The output of objective functions in case of worst and best answers is arranged in the order of the nadir point f_n^{SN} and ideal point f_n^u. The optimality of the objective function is indicated by μ_n^r in the r-th Pareto solution number. μ_n^r is the membership function f_n in the r-th Pareto solution number, and f_n^r is the expression of the value of the objective function f_n in the r-th Pareto solution number. The general membership function of the r-th Pareto solution is called μ^r, which is calculated according to (46), where ω_n is the importance factor of the n-th objective function. Decision-maker is the responsible for the values of the importance coefficients. For example, if environmental issues are the decision-maker's top priority, f_1 will be given a lower value, and if financial issues are more important, f_1 will be given a higher value [43]. The best solution is the one with the highest amount of μ_r.

Table 1: MT information [41].

MT location	Maximum power (kW)	Incremental rate (kW)	Reduction rate (kW)	Minimum on time (hours)	Minimum downtime (hours)	Minimum uptime (hours)	Initial condition of MTs	Start-up and shutdown cost ($)	φ_i (kg/kW)
15	800	250	250	250	2	2	1	3	0.012
18	650	250	250	250	2	2	1	3	0.03
19	100	100	100	100	2	2	0	3	0.075
25	750	250	250	250	2	2	0	3	0.035
29	750	250	250	250	2	2	1	3	0.035

(1) Maximization:

$$\mu_n^r = \begin{cases} 0, & f_n^r \le f_n^{\mathrm{SN}}, \\ \dfrac{f_n^r - f_n^{\mathrm{SN}}}{f_n^u - f_n^{\mathrm{SN}}} & f_n^{\mathrm{SN}} \le f_n^r \le f_n^u, \\ 1, & f_n^r \ge f_n^u, \end{cases} \tag{44}$$

$$n = 1.$$

(2) Minimization:

$$\mu_n^r = \begin{cases} 1, & f_n^r \le f_n^u, \\ \dfrac{f_n^{\mathrm{SN}} - f_n^r}{f_n^{\mathrm{SN}} - f_n^u} & f_n^u \le f_n^r \le f_n^{\mathrm{SN}}, \\ 0, & f_n^r \ge f_n^{\mathrm{SN}}, \end{cases} \tag{45}$$

$$n = 2,$$

$$\mu_r = \frac{\sum_{n=1}^{P} \omega_n \cdot \mu_n^r}{\sum_{n=1}^{P} \omega_n}. \tag{46}$$

Both models are mixed-integer linear programming problems and are solved in GAMS software with the powerful CPLEX solver.

4. Case Studies

The simulation is performed on an IEEE 33-bus system to validate the proposed scheme, as shown in Figure 2 [41]. The information about the ESS and DG resources used is shown in Table 2 [41]. In the studied system, the power of each residential house is assumed to be 10 kW. The smart devices inside each house are divided into adjustable, interruptible, and deferrable (shiftable) devices. For home appliances, uncontrollable appliances are considered 0.8 kW. Also, 3.5 kW of the total power of equipment with first priority, 3.1 kW of equipment with second priority, and 2.6 kW of equipment with third priority are assumed for each house [45]. Table 1 shows the MT information. Information on the wind, solar, and load coefficients and energy prices are shown in Figures 3 and 4, respectively. Table 3 shows the costs associated with the model parameters. Problems are solved in two case studies, single objective and multiobjective.

4.1. The Single-Objective Solution to the Problem. In this case, the emission is not considered. A fault between buses 4 and 5 is considered for testing the proposed model in the first layer. Figure 5 shows the optimal system arrangement after fault between buses 4 and 5 (first layer output). Since the aim is to island the faulty area, connecting tie switches 33, 35, and 37 is impossible. Because by connecting these switches, the MG no longer acts as an island. Four island MGs are formed in the faulty area after isolating the line between buses 4 and 5. The first MG is shown in pink, the second MG in red, the third MG in green, and the fourth MG in blue. Tie switches 34 and 36 are closed. Switches 7, 10, 15, 16, and 31 are also open. As seen in Figure 6, the radiality condition of the faulty area is maintained.

According to the optimal arrangement in layer 1, the unit commitment problem is implemented in the second layer. The output results for the second layer are shown in Table 4. The first point in Table 4 is that the MTs connected to the upstream network (19, 25) have no output. According to the energy price shown in Figure 7 at 19:00 and 20:00, it may be seen that the energy price in these two hours is less than 0.1 $/kWh. Since the generation cost of MTs is estimated at 0.1 $/kWh, the program prefers to purchase electricity from the upstream network instead of utilizing MTs to decrease operation costs. However, other MTs have outputs with the capacity specified in Table 4. The second point is that the MT 5 in MG 1 is charged (its battery) in this state, which is not logical (due to the emergency state). The reason for charging battery 5 is that the minimum amount of battery 5 is 30 kW, while the initial charge status of battery 5 is 15 kW. Due to the minimum amount of the battery, in this situation, battery 5 reaches its minimum charge (30 kW) by charging 15.789 kW at 19:00. The rest of the batteries are discharged until the minimum battery charge is reached. No interruptions occurred at 19:00 and 20:00. To reduce operating costs, the load shedding is 913,513 kW at 19:00 and 1012.724 kW at 20:00.

Figures 5 and 7 show priorities 2 and 3 of load shedding per bus, respectively. Since priority 1 of load shedding is of the highest importance, and the highest cost of load shedding in the DR program, no priority 1 of load-shedding has been shed at 19:00 and 20:00. Priority 3 of load shedding has the lowest value due to its lower importance. Therefore,

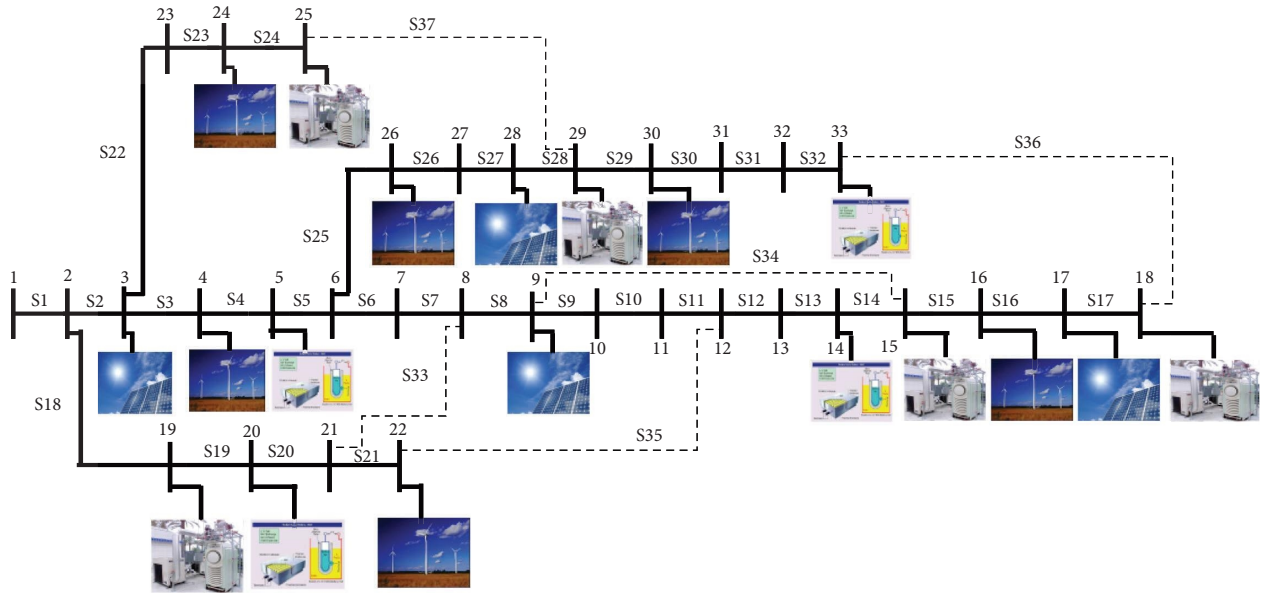

Figure 2: Test system [41].

Table 2: Information on DG and battery resources [41].

ESS			PV			WT	
ESS location	Minimum charge	Power (kW)	PV location	Initial charge	Power (kW)	Location WT	Power (kW)
5	0.2	150	3	0.1	60	4	30
14	0.2	15	9	0.9	60	16	85
20	0.2	200	17	0.8	40	22	60
33	0.2	200	28	0.5	50	24	50
						26	50
						30	70

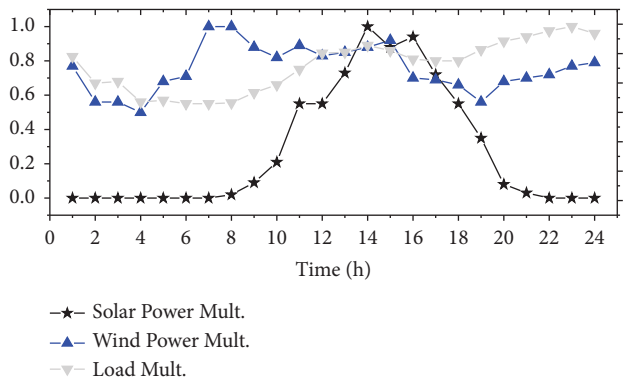

Figure 3: Wind, solar, and load coefficients [41].

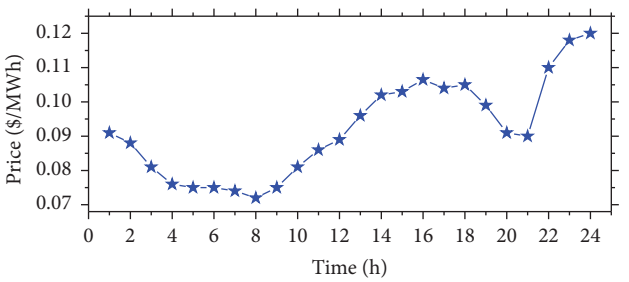

Figure 4: Energy prices [41].

Table 3: Parameters for calculating the relevant costs [41, 45].

Parameters	Value ($/MWh)
C^G	0.1
C^D	0.3
C^{emi}	0.02
C^{LS4}	5
C^{LS1}	3.5
C^{LS2}	3
C^{LS3}	2.2

according to Figure 7, the load shedding in these loads has occurred in the highest amount. According to Figure 5, priority 2 of load shedding is higher in different buses. In Figures 5 and 7, buses 24 and 25 have the highest load-shedding rates (because these two buses have a large load).

The proposed model is compared with the results of [41] to validate the results. The execution time of the proposed method is lower than [41] (and all studies that have used the nonlinear model in this layer). The technique used by [41] and most of the methods in the literature are not practically applicable to large systems. In contrast, the proposed scheme performs any system in the shortest possible time. The second advantage of the proposed scheme is to reduce the

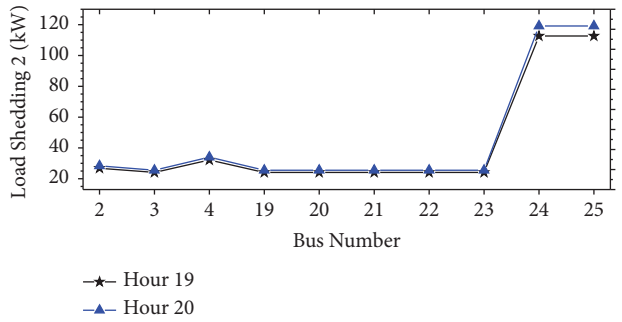

Figure 5: Priority 2 of load shedding.

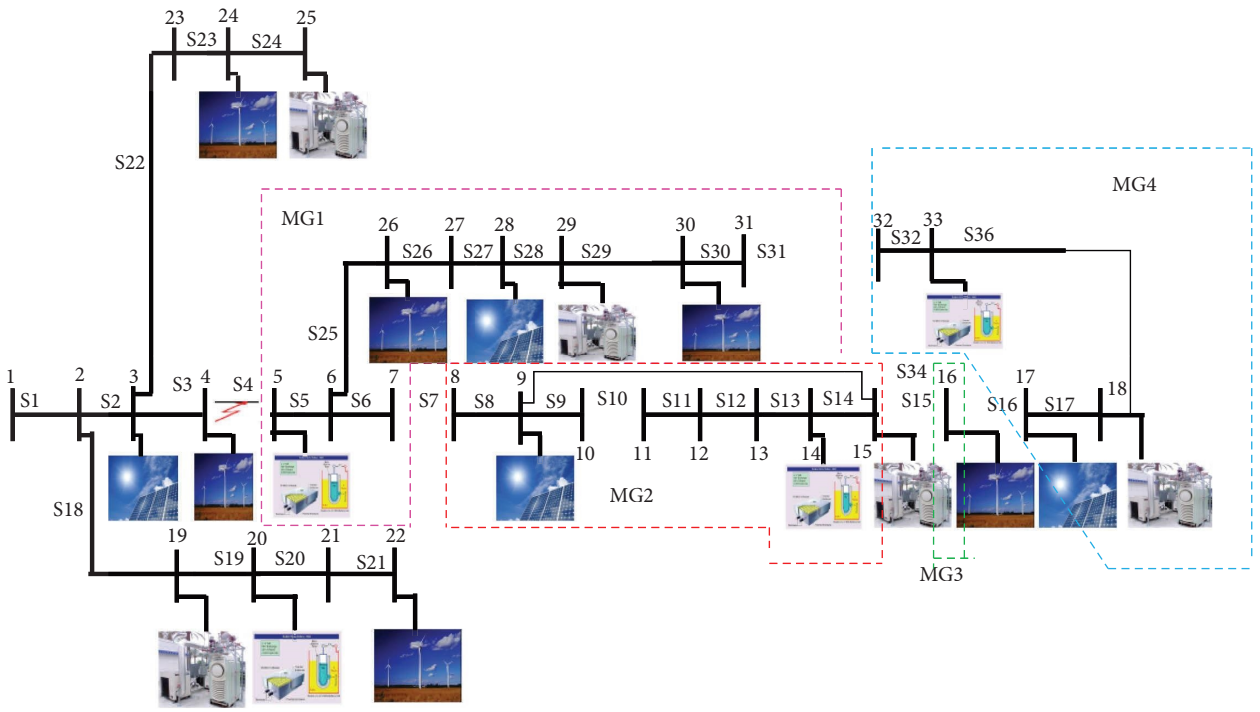

Figure 6: Optimal system arrangement after fault between buses 4 and 5 (first layer output).

Table 4: Second layer results from fault between buses 4 and 5.

Time	Optimal load planning		Nondispatchable resources planning			
	Load shedding Power (kW)	Load outage Power (kW)	SOC	Power (kW)	Bus	Network sections
19:00	913.513	—	—	434.112	Exchange	Section connected to the upstream
			91.452	61.693	ES20	
			30	−15.789	ES5	MG 1
			—	650	MT29	
			106.667	39	ES14	MG 2
			—	511.743	MT15	
			—	349.3	MT18	MG 4
20:00	1012.724	—	—	515.188	Exchange	Section connected to the upstream
			40	46.307	ES20	
			—	650	MT29	MG 1
			—	554.394	MT15	MG 2
			30	69	ES14	
			—	338.7	MT18	MG 4
			40	54	ES33	

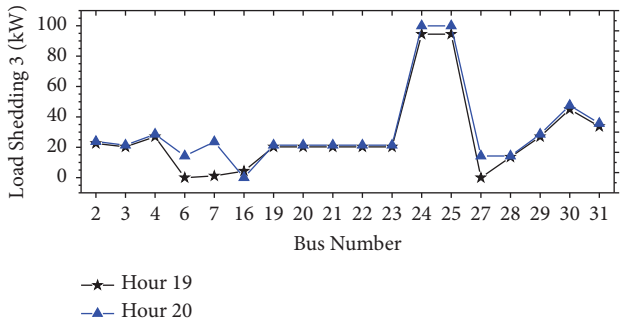

Figure 7: Priority 3 of load shedding.

Table 5: Comparison of results with the study in [41].

	Execution time of layer 1 (s)	Load shedding (kW)	Number of MG	Number of switches
Proposed method	1	1926.237	4	8
Reference [41]	15.3	2030.963	2	12

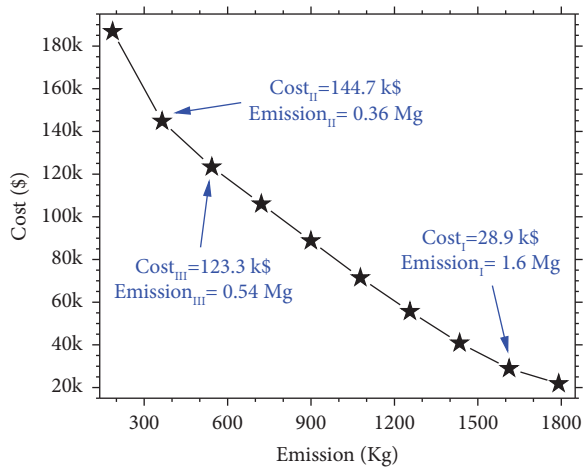

Figure 8: Pareto optimal solutions, the cost versus emission.

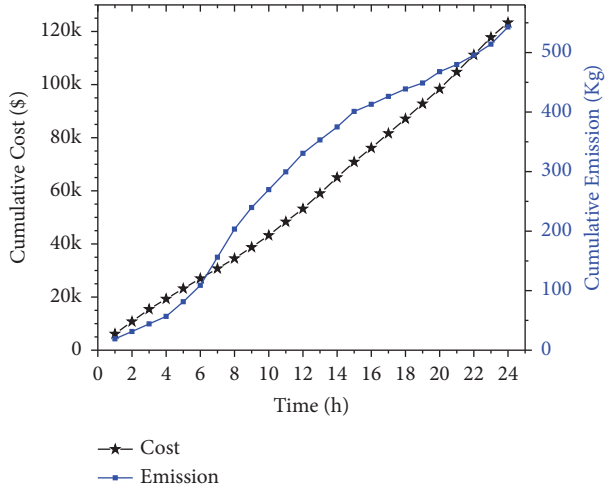

Figure 9: Cumulative cost and emission of the smart distribution system.

number of switches. In [41], 12 switching operations have occurred.

In contrast, in the proposed approach, the number of switches is 8. The number of MGs formed is 4 and 2 for the proposed approach and the study in [41], respectively. Also, the total load shedding in the proposed approach in the self-healing period is 104.726 less than the study in [41]. Therefore, the proposed approach in this study has a considerable advantage over the existing methods in the literature. In order to validate the results of the proposed method, the comparison of the present study with the study in [41] is mentioned in Table 5.

4.2. Solving the Two-Objective Problem of Cost and Emission in the Smart Distribution System Using the Epsilon Constraint Method. In order to solve the problem, the two-objective method has been used. The first objective function is considered the main objective function (f_1), and the second objective function, i.e. emission, is considered the problem constraint (f_2). The problem is solved based on the equations mentioned earlier. As shown in Figure 8, the amount of emission and the cost are inversely related. As one increases, the other decreases. This is because in order to have less emission, it is necessary to use more units that are more expensive and produce less emission.

First, to solve the epsilon-constraint method, the problem is solved as a single objective by considering the cost. In this case, the cost is at its lowest (21,811.972 $), and the emission is at its highest (1,790.768 kg). Then, the problem is solved as a single objective by only considering the emission. In this case, the emission is at its lowest value (186.472 kg), and the cost is at its highest (189,082.811 $). Then, to generate Pareto solutions, the model is solved as a single-objective problem by considering the cost as a main objective function and emission as a subobjective function

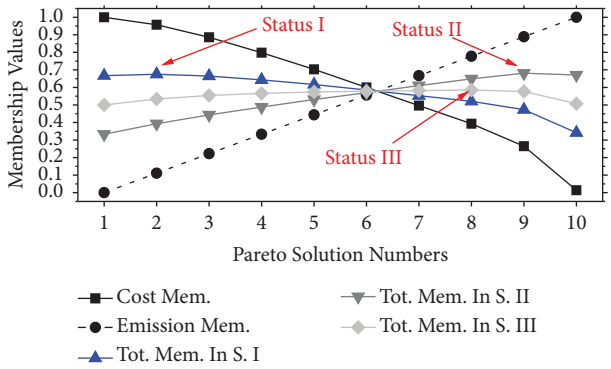

FIGURE 10: Variation of the total membership and cost and emission functions versus Pareto optimal solutions.

(constraint). The problem is solved this way, and 10 Pareto solutions are generated, as shown in Figure 9.

The fuzzy method is used to select the best solution. On the other hand, this problem is solved in three different categories.

Category I: the importance factor of the cost objective function is considered to be double the emission one

Category II: the importance factor of the emission objective function is considered to be double the cost

Category III: the importance factor of the cost objective function is considered equal to the emission one

According to the expressed categories and as shown in Figure 10, the best Pareto solution is obtained in each category. The second Pareto solution is selected as the best one in category I. The ninth and eighth Pareto solutions are chosen as the best solutions in category II and III, respectively. Figure 8 shows the cost and emission of these Pareto solutions, and Figure 10 shows their membership values.

Figure 9 shows the cost and emission cumulatively for 24 hours.

5. Conclusion

Distribution system restoration is one of the steps of self-healing smart distribution systems. After isolating the fault, restoration has two stages, including restoration and unit commitment. One of the challenges for researchers to solve the restoration problem in large-scale distribution systems is the considerable time to solve the problem. This study presents a new linear model for solving the postfault restoration problem, which significantly reduces the time and ensures the optimal solution due to mathematical solvers. In the first layer, the faulty area is transformed into one or multi-island-operating MGs. Optimal island-operating MGs after the fault is one of the essential advantages of the proposed scheme.

Furthermore, in the second layer, using the new arrangement in the first step, the problem of unit commitment in a smart distribution system is solved by a linear model. This study uses ES and various dispatchable and nondispatchable generations, along with DR tools. Controllable loads are divided into adjustable loads and interruptible and shiftable loads to exploit the DR tool. Using DR schemes in self-healing mode reduces system operating costs. Comparing the presented numerical results with existing methods ensures the excellent performance of the proposed method. Another goal of this paper is to use multiobjective modeling and the epsilon constraint method to minimize the cost and emission of the system. The results indicated that, in the multiobjective model, we should have a trade-off between cost and emission to have an appropriate solution among Pareto solutions.

Nomenclature

Sets

i, j: Set of nodes
t: Set of times
k: Set of nodes in first layer

Parameters

$P_{i,t}^{D}$:	Active power of the loads
$P_{i,t}^{\mathrm{WT}}$:	Active power of WT
$P_{i,t}^{\mathrm{PV}}$:	Active power of PV
$G_{i,j}$:	Conductance of lines
C^{G}:	Cost of generation
C^{LS1}:	Cost of load shedding with priority 1
$\mathrm{Pload1}_{i,t}^{D}$:	The total active power for priority 1 of loads
$\mathrm{Pload2}_{i,t}^{D}$:	The total active power for priority 2 of loads
$\mathrm{Pload3}_{i,t}^{D}$:	The total active power for priority 3 of loads
$\mathrm{Pload4}_{i,t}^{D}$:	The total active power of noncontrollable loads
C_{t}^{b}:	Price of buying from the upstream network
Δv:	The amount of allowable voltage changes in the distribution network
$S_{i}^{\max}$:	The maximum apparent power of MTs
π_{c}:	The efficiency of the ESS charge
π_{d}:	The efficiency of the ESS discharge
EC_{i}:	The capacity of ESS
SDC/STC:	Shutdown/start-up cost of MTs
$B_{i,j}$:	Susceptance of lines
$\mathrm{RD}_{i}/\mathrm{RU}_{i}$:	Ramp-down/ramp-up of MTs
$\mathrm{SD}_{i}/\mathrm{SU}_{i}$:	Ramp limit for shutdown/start-up of MTs
C_{t}^{s}:	Price of selling electricity to the upstream network
C^{D}:	Profit from the sale of electricity
C^{LS2}:	Cost of load shedding with priority 2
C^{LS3}:	Cost of load shedding with priority 3
C^{LS4}:	Cost of load outage
$a_{i}^{G}, b_{i}^{G}, c_{i}^{G}$:	Fuel cost function coefficients
U_{i}^{0}/S_{i}^{0}:	The on/off duration of unit i at the beginning of the investigated period (end of $t=0$)
$P_{i}^{\mathrm{ch,max}}/P_{i}^{\mathrm{dch,max}}$:	Maximum charge/discharge power of ESS
$\mathrm{SOC}_{i}^{\max}$:	Maximum SOC of ESS
$\mathrm{UT}_{i}/\mathrm{DT}_{i}$:	Minimum up-time/down-time of MTs

$\underline{pg}_{(i,t)}/\overline{pg}_{(i,t)}$: Minimum/maximum output power of MTs
T: Number of hours of the planning period

Variables

$P_{i,t}$: The active power flow
$p^G_{i,t}$: The total amount of active power generation
$p^E_{i,t}$: The amount of power to charge or discharge ESS
PLS1: Priority 1 of load shedding
$\theta_{ij,t}$: Angle between voltage bus i and j in hour t
PLS2: Priority 2 of load shedding
PLS3: Priority 3 of load shedding
$\Delta V_{i,t}/\Delta V_{j,t}$: The amount of voltage changes
S_i: Apparent power
$V_{i,t}$: Bus voltage
$\phi_{i,t}/\lambda_{i,t}$: Binary variable for discharge/charge ESS
$z_{i,t}/y_{i,t}$: Binary variable for shutdown/start-up of MTs
$u_{i,t}$: Binary variable to indicate the up or down status of MTs
$Cs_{i,t}$: Binary variable to determine the buses that are omitted
PLS4: Load outage
λ_t: Selling power to the upstream network
μ_t: Buying power from the upstream network
$SOC_{i,t}$: State of charge of ESS.

Data Availability

The data used to support the findings of this study are available from the corresponding author upon request.

Conflicts of Interest

The authors declare that there are no conflicts of interest.

References

[1] S. Massoud Amin and B. F. Wollenberg, "Toward a smart grid: power delivery for the 21st century," *IEEE Power and Energy Magazine*, vol. 3, no. 5, pp. 34–41, 2005.

[2] D. Sarathkumar, "A technical review on self-healing control strategy for smart grid power systems," in *Proceedings of the IOP Conference Series: Materials Science and Engineering*, IOP Publishing, Bristol, United Kingdom, February 2021.

[3] N. Meenakshi and D. Kavitha, "Optimized self-healing of networked microgrids using differential evolution algorithm," in *Proceedings of the 2018 National Power Engineering Conference (NPEC)*, March 2018.

[4] E. Drayer, N. Kechagia, J. Hegemann, M. Braun, M. Gabel, and R. Caire, "Distributed self-healing for distribution grids with evolving search space," *IEEE Transactions on Power Delivery*, vol. 33, no. 4, pp. 1755–1764, 2018.

[5] J. B. Leite and J. R. S. Mantovani, "Development of a self-healing strategy with multiagent systems for distribution networks," *IEEE Transactions on Smart Grid*, vol. 8, no. 5, pp. 2198–2206, 2017.

[6] A. Golshani, W. Sun, Q. Zhou, Q. P. Zheng, and J. Tong, "Two-stage adaptive restoration decision support system for a self-healing power grid," *IEEE Transactions on Industrial Informatics*, vol. 13, no. 6, pp. 2802–2812, 2017.

[7] S. S. Refaat, A. Mohamed, and P. Kakosimos, "Self-Healing control strategy; Challenges and opportunities for distribution systems in smart grid," in *Proceedings of the 2018 IEEE 12th International Conference on Compatibility, Power Electronics and Power Engineering (CPE-POWERENG 2018)*, April 2018.

[8] L. H. Leite, "Self-healing in distribution grids supported by photovoltaic dispersed generation in a voltage regulation perspective," in *Proceedings of the 2019 IEEE PES Innovative Smart Grid Technologies Conference-Latin America (ISGT Latin America)*, IEEE, Gramado, Brazil, September 2019.

[9] M. N. Ambia, K. Meng, W. Xiao, and Z. Y. Dong, "Nested formation approach for networked microgrid self-healing in islanded mode," *IEEE Transactions on Power Delivery*, vol. 36, no. 1, pp. 452–464, 2021.

[10] S. Ma, A. Arif, and Z. Wang, "Resilience assessment of self-healing distribution systems under extreme weather events," in *Proceedings of the 2019 IEEE Power and Energy Society General Meeting (PESGM)*, Atlanta, GA, USA, August 2019.

[11] M. Çinar and A. Kaygusuz, "Self-healing in smart grid: a review," *Bitlis Eren Üniversitesi Fen Bilimleri Dergisi*, vol. 7, no. 2, pp. 492–503, 2018.

[12] V. Hosseinnezhad, M. Rafiee, M. Ahmadian, and P. Siano, "A comprehensive framework for optimal day-ahead operational planning of self-healing smart distribution systems," *International Journal of Electrical Power and Energy Systems*, vol. 99, pp. 28–44, 2018.

[13] N. Nikmehr, S. Najafi-Ravadanegh, and A. Khodaei, "Probabilistic optimal scheduling of networked microgrids considering time-based demand response programs under uncertainty," *Applied Energy*, vol. 198, pp. 267–279, 2017.

[14] A. Ghasemi and M. Enayatzare, "Optimal energy management of a renewable-based isolated microgrid with pumped-storage unit and demand response," *Renewable Energy*, vol. 123, pp. 460–474, 2018.

[15] R. Deng, Z. Yang, M. Y. Chow, and J. Chen, "A survey on demand response in smart grids: mathematical models and approaches," *IEEE Transactions on Industrial Informatics*, vol. 11, no. 3, pp. 570–582, 2015.

[16] H. Haddadian and R. Noroozian, "Multi-microgrid-based operation of active distribution networks considering demand response programs," *IEEE Transactions on Sustainable Energy*, vol. 10, no. 4, pp. 1804–1812, 2019.

[17] S. E. Ahmadi and N. Rezaei, "A new isolated renewable based multi microgrid optimal energy management system considering uncertainty and demand response," *International Journal of Electrical Power and Energy Systems*, vol. 118, Article ID 105760, 2020.

[18] Y. Wang, Y. Huang, Y. Wang et al., "Energy management of smart micro-grid with response loads and distributed generation considering demand response," *Journal of Cleaner Production*, vol. 197, pp. 1069–1083, 2018.

[19] A. Mehdizadeh, N. Taghizadegan, and J. Salehi, "Risk-based energy management of renewable-based microgrid using information gap decision theory in the presence of peak load management," *Applied Energy*, vol. 211, pp. 617–630, 2018.

[20] R. S. Netto, G. Ramalho, B. Bonatto et al., "Real-time framework for energy management system of a smart microgrid using multiagent systems," *Energies*, vol. 11, no. 3, p. 656, 2018.

[21] W.-Y. Chiu, J.-T. Hsieh, and C.-M. Chen, "Pareto optimal demand response based on energy costs and load factor in smart grid," *IEEE Transactions on Industrial Informatics*, vol. 16, no. 3, pp. 1811–1822, 2020.

[22] H. Mehrjerdi and R. Hemmati, "Coordination of vehicle-to-home and renewable capacity resources for energy management in resilience and self-healing building," *Renewable Energy*, vol. 146, pp. 568–579, 2020.

[23] S. Mohsen, "Enhancement of self-healing property of smart grid in islanding mode using electric vehicles and direct load control," in *Proceedings of the 2014 Smart Grid Conference (SGC)*, December 2014.

[24] M. Mahdi and V. M. I. Genc, "A real-time self-healing methodology using model-and measurement-based islanding algorithms," *IEEE Transactions on Smart Grid*, vol. 10, no. 2, pp. 1195–1204, 2019.

[25] M. Yang, J. Wang, and J. An, "Day-ahead optimization scheduling for islanded microgrid considering units frequency regulation characteristics and demand response," *IEEE Access*, vol. 8, pp. 7093–7102, 2020.

[26] W. Sun, S. Ma, I. Alvarez-Fernandez, R. Roofegari nejad, and A. Golshani, "Optimal self-healing strategy for microgrid islanding," *IET Smart Grid*, vol. 1, no. 4, pp. 143–150, 2018.

[27] R. Rahmani and A. Fakharian, "New control method of islanded microgrid system: a GA and ICA based optimization approach," *The Modares Journal of Electrical Engineering*, vol. 12, no. 4, pp. 40–49, 2016.

[28] L. Sedghi, M. Emam, A. Fakharian, and M. Savaghebi, "Decentralized control of an islanded microgrid based on offline model reference adaptive control," *Journal of Renewable and Sustainable Energy*, vol. 10, no. 6, 2018.

[29] M. K. Sharma, P. Kumar, and V. Kumar, "Intentional islanding of microgrid," in *Proceedings of the 2017 6th International Conference on Computer Applications in Electrical Engineering-Recent Advances (CERA)*, IEEE, Roorkee, India, October 2017.

[30] D. Li, W. Shouxiang, Z. Jie, and Z. Yishu, "A self-healing reconfiguration technique for smart distribution networks with DGs," in *Proceedings of the 2011 International Conference on Electrical and Control Engineering*, September 2011.

[31] M. F. Zia, E. Elbouchikhi, M. Benbouzid, and J. M. Guerrero, "Energy management system for an islanded microgrid with convex relaxation," *IEEE Transactions on Industry Applications*, vol. 55, no. 6, pp. 7175–7185, 2019.

[32] A. Jafari, H. Ganjeh Ganjehlou, T. Khalili, and A. Bidram, "A fair electricity market strategy for energy management and reliability enhancement of islanded multi-microgrids," *Applied Energy*, vol. 270, Article ID 115170, 2020.

[33] M. H. Andishgar, E. Gholipour, and R.-A. Hooshmand, "An overview of control approaches of inverter-based microgrids in islanding mode of operation," *Renewable and Sustainable Energy Reviews*, vol. 80, pp. 1043–1060, 2017.

[34] K. Balasubramaniam, P. Saraf, R. Hadidi, and E. B. Makram, "Energy management system for enhanced resiliency of microgrids during islanded operation," *Electric Power Systems Research*, vol. 137, pp. 133–141, 2016.

[35] W. Alharbi and K. Bhattacharya, "Demand response and energy storage in MV islanded microgrids for high penetration of renewables," in *Proceedings of the 2013 IEEE Electrical Power and Energy Conference*, August 2013.

[36] B. S. K. Patnam and N. M. Pindoriya, "Demand Response in Consumer-Centric Electricity Market: Mathematical Models and Optimization Problems," *Electric Power Systems Research*, vol. 193, Article ID 106923, 2020.

[37] S. Raza, T. ur Rahman, M. Saeed, and S. Jameel, "Performance analysis of power system parameters for islanding detection using mathematical morphology," *Ain Shams Engineering Journal*, vol. 12, no. 1, pp. 517–527, 2021.

[38] M. A. Farhan and K. Shanti Swarup, "Mathematical morphology-based islanding detection for distributed generation," *Institution of Engineering and Technology Generation, Transmission and Distribution*, vol. 10, no. 2, pp. 518–525, 2016.

[39] P. L. Cavalcante, J. C. Lopez, J. F. Franco et al., "Centralized self-healing scheme for electrical distribution systems," *IEEE Transactions on Smart Grid*, vol. 7, no. 1, pp. 145–155, 2016.

[40] Z. Wang and J. Wang, "Self-healing resilient distribution systems based on sectionalization into microgrids," *IEEE Transactions on Power Systems*, vol. 30, no. 6, pp. 3139–3149, 2015.

[41] M. Zadsar, M. R. Haghifam, and S. M. Miri Larimi, "Approach for self-healing resilient operation of active distribution network with microgrid," *IET Generation, Transmission and Distribution*, vol. 11, no. 18, pp. 4633–4643, 2017.

[42] K. Choopani, M. Hedayati, and R. Effatnejad, "Self-healing optimization in active distribution network to improve reliability, and reduction losses, switching cost and load shedding," *International Transactions on Electrical Energy Systems*, vol. 30, no. 5, Article ID e12348, 2020.

[43] M. Shafiekhani, A. Ahmadi, O. Homaee, M. Shafie-khah, and J. P. Catalao, "Optimal bidding strategy of a renewable-based virtual power plant including wind and solar units and dispatchable loads," *Energy*, vol. 239, Article ID 122379, 2022.

[44] M. Shafiekhani, A. Badri, M. Shafie-Khah, and J. P. Catalão, "Strategic bidding of virtual power plant in energy markets: a bi-level multi-objective approach," *International Journal of Electrical Power and Energy Systems*, vol. 113, pp. 208–219, 2019.

[45] S. Sanaei, M. R. Haghifam, and A. Safdarian, "Centralized optimal management of a smart distribution system considering the importance of load reduction based on prioritizing smart home appliances," *Institution of Engineering and Technology Generation, Transmission and Distribution*, vol. 16, no. 19, pp. 3874–3893, 2022.